HHS Public Access

Author manuscript

Neuroscience. Author manuscript; available in PMC 2017 March 01.

Published in final edited form as:

Neuroscience. 2016 March 1; 316: 151–166. doi:10.1016/j.neuroscience.2015.12.030.

Topographic organizations of taste-responsive neurons in the parabrachial nucleus of C57BL/6J mice: an electrophysiological mapping study

Kenichi Tokita[1,*] and **John D. Boughter Jr.**[1]

[1]Department of Anatomy & Neurobiology, University of Tennessee Health Science Center, 855 Monroe Avenue, Suite 515, Memphis, TN 38163, USA.

Abstract

The activities of 178 taste-responsive neurons were recorded extracellularly from the parabrachial nucleus (PbN) in the anesthetized C57BL/6J mouse. Taste stimuli included those representative of 5 basic taste qualities, sweet, salty, sour, bitter and umami. Umami synergism was represented by all sucrose-best and sweet-sensitive sodium chloride-best neurons. Mediolaterally the PbN was divided into medial, brachium conjunctivum (BC) and lateral subdivisions while rostrocaudally the PbN was divided into rostral and caudal subdivisions for mapping and reconstruction of recording sites. Neurons in the medial and BC subdivisions had a significantly greater magnitude of response to sucrose and to the mixture of monopotassium glutamate and inosine monophosphate than those found in the lateral subdivision. In contrast, neurons in the lateral subdivision possessed a more robust response to quinine hydrochloride. Rostrocaudally no difference was found in the mean magnitude of response. Analysis on the distribution pattern of neuron types classified by their best stimulus revealed that the proportion of neuron types in the medial vs. lateral and BC vs. lateral subdivisions was significantly different, with a greater amount of sucrose-best neurons found medially and within the BC, and a greater amount of sodium chloride-, citric acid- and quinine hydrochloride-best neurons found laterally. There was no significant difference in the neuron type distribution between rostral and caudal PbN. We also assessed breadth of tuning in these neurons by calculating entropy (*H*) and noise-to-signal (N/S) ratio. Mean N/S ratio of all neurons (0.43) was significantly lower than that of *H* value (0.64). Neurons in the caudal PbN had a significantly higher *H* value than in the rostral PbN. In contrast, mean N/S ratio were not different both mediolaterally and rostrocaudally. These results suggest that although there is overlap in taste quality representation in the mouse PbN, taste-responsive neurons still possessed a topographic organization.

Keywords

Taste; Parabrachial; Topography; Electrophysiology; Umami; Mouse

[*]Corresponding author, Kenichi Tokita, Present address, Laboratory for Affiliative Social Behavior, RIKEN Brain Science Institute, 2-1 Hirosawa, Wako-shi, Saitama 351-0198, Japan, Phone: +81-48-462-1111, Fax: +81-48-467-6947, kenichi.tokita@riken.jp.

Introduction

A fundamental issue in neuroscience is to understand how sensory information is structured within neural space in the central nervous system. Topographic organization involves the perpetuation of information between brain areas, organized in adjacent cells with similar physiological functions and anatomical connections (Thivierge and Marcus, 2007). Topography often refers to a neuronal "map" corresponding to receptor location on the body surface, and this organization is seen clearly in the somatosensory and visual systems (e.g. Butler and Hodos, 1996; Kaas, 1997). However, topographical organization does not necessarily have to be spatial in nature, or reflect body surface. For example, the auditory system utilizes tonotopic organization, a neuronal representation of frequency. In the olfactory system, functionally distinct populations of olfactory neurons project to specific glomeruli within the olfactory bulb (e.g. Mori et al., 2006). Location in the olfactory epithelium is only crudely represented in the olfactory bulb (i.e. dorsal vs. ventral); instead, it is odor uniqueness or similarity that is organized in the pattern of olfactory neuron–glomeruli connections.

Although individual taste qualities may activate specific taste receptor cells, the distribution of these types of receptor cells largely overlaps within taste buds, and throughout the oral cavity (e.g. Chandrashekar et al., 2006; Chaudhari and Roper, 2010). However, there is still at least crude somatotopy (called "orotopy") in the afferent nerves and CNS, based on the fact that taste information from the anterior tongue, palate, posterior tongue and epiglottis is carried in four separate nerves, which terminate in the nucleus of the solitary tract (NST) along a rostral-caudal gradient (although the terminal fields have a degree of overlap; for reviews, see Lundy and Norgren, 2015; Whitehead, 2012). This rough organization according to receptive field location has been confirmed in both single unit (Sweazey and Smith, 1987; Travers and Norgren, 1995; Geran and Travers, 2006) as well as multi-unit (Halpern and Nelson, 1965; Dickman and Smith, 1989) *in vivo* electrophysiological studies. Whether there is also central organization based on quality (i.e. sweet, salty, sour, bitter and umami) is less clear. In the NST, there is general agreement from physiological and neuroanatomical studies with rodents that there is some degree of segregation of primary tastes, especially sweet vs. bitter (Harrer and Travers, 1996; Sugita and Shiba, 2005; Travers et al., 2007; Stratford and Finger, 2011; Yokota et al., 2014).

The parabrachial nucleus (PbN) is the second gustatory relay in rodents, and comprises a key interface between brainstem and forebrain gustatory and visceral areas (Tokita et al., 2009, 2010, 2014; Magableh and Lundy, 2014). Despite substantial overlap of inputs from taste and visceral regions of the NST (Karimnamazi et al., 2002), the crude somatotopy of taste responses in the oral cavity appears to be maintained in this nucleus. Halsell and Travers (1997) showed electrophysiologically in the rat that gustatory neurons in the caudal PbN are more responsive to taste stimuli presented in the anterior oral cavity than posterior oral cavity. Cells activated by posterior stimulation were found more rostrally. Segregation according to taste quality is less clear; Ogawa et al. (1987) showed that sodium chloride-best neurons were preferentially found caudal and ventral, while hydrochloric acid-best cells were found rostral and dorsal in the rat PbN. A classic c-Fos immunohistochemical study by

Yamamoto et al. (1994) suggested that taste quality and hedonics might be represented by different subnuclei in the rat PbN.

Only few *in vivo* electrophysiological investigations into the topographic representation of taste in the PbN have been performed in the mouse, an experimental model species with an increasing importance in the field. In two previous single-unit recording studies from our lab (Tokita et al., 2012; Tokita and Boughter, 2012) we collected taste responses from 52 and 70 PbN neurons, respectively. These sample sizes are similar to the other few published studies of mouse taste brainstem (NST) physiology using *in vivo* methods (e.g. McCaughey, 2007; Lemon and Margolskee, 2009; Wilson et al., 2012). When recording sites were reconstructed and plotted, we found only a significant propensity for more cells classified as sweet-best to be located medially in the PbN. However, if topographic distribution by primary quality is subtle in nature, or based on other functional properties of taste neurons (such as breadth of response), a robust dataset is needed to better examine this question.

In the present study, a total of 56 taste-responsive neurons were isolated, and responses to a battery of basic taste stimuli recorded. We combined these data with 122 neurons collected in our previous studies (Tokita et al., 2012; Tokita and Boughter, 2012). We included the fifth basic taste umami as one of the stimuli used in the present study, including both individual stimuli and a synergistic mix, as umami was typically omitted in previous electrophysiological mapping studies in the rat and hamster.

Experimental Procedures

Subjects

Data were collected from 82 adult male C57BL/6J mice (17–33 g, aged 3 to 4 months) which were originally obtained from the Jackson Laboratory (Bar Harbor, ME, USA) and were bred in our colony. Of these subjects, 60 mice were used in our previous studies (Tokita et al., 2012; Tokita and Boughter 2012), and 22 mice were used for collection of additional data for the present study. The animals were maintained in a temperature- and humidity-controlled vivarium on a 12:12 h light-dark cycle (lights on at 0700 h, off at 1900 h), and were given free access to food (22/5 rodent diet, Harlan Teklad, Madison, WI, USA) and water. This study was approved by the Animal Care and Use Committee at UTHSC, and all experiments were carried out in accordance with the National Institute of Health Guide for Care and Use of Laboratory Animals (NIH Publications No. 80–23), revised 1996.

Surgery

Animals were anesthetized with intraperitoneal injection of urethane (ethyl carbamate) (1 g/kg) followed by extra doses as necessary throughout the experiment. After tracheal cannulation (PE60 polyethylene tubing, Intramedic, Becton Dickson, Parsippany, NJ, USA) to create a surgical airway, each mouse was fixed in a stereotaxic apparatus equipped with non-traumatic headholder (Stoelting, Wood Dale, IL, USA) that angled bregma and lambda level. Body temperature was monitored and maintained at 35 °C using a heating pad (Elenco electronics, Wheeling, IL, USA). The scalp was opened with a midline incision, and a hole (approximately 4.0 mm in diameter, just posterior to the lambda) was drilled through the

skull to expose the surface of the cerebellum and inferior colliculus. The dura mater covering the inferior colliculus was removed to allow easier access to the PbN.

Test solutions

Taste stimuli presented to 22 mice were 0.5 M sucrose (sweet), 0.1 M sodium chloride (salty, NaCl), 0.01 M citric acid (sour), 0.01 M quinine hydrochloride (bitter, QHCl), 0.1 M monopotassium glutamate (umami, MPG), 0.01 M inosine 5'-monophosphate (umami, IMP), and a mixture of 0.1 M MPG and 0.01 M IMP. All of these tastants were included in our previous studies (Tokita et al., 2012; Tokita and Boughter, 2012), and neural data for these stimuli were selected and combined together in the present study. MPG was used instead of monosodium glutamate (MSG) to more clearly show umami mixture synergism by precluding the substantial effect of the sodium ion on gustatory neural responses (Yamamoto et al., 1991; Sako et al., 2003). Taste solutions were made from reagent-grade chemicals dissolved in distilled water and presented at room temperature during testing.

Electrophysiological recording

To locate the gustatory zone of the mouse PbN, the inferior colliculus, just posterior to the transverse sinus on the dorsal surface of the exposed tissue, was used as a landmark. Unlike other rodent model animals such as rats and hamsters, vertical access to the PbN was possible in mice, and this made it possible to more reliably reconstruct recording sites in the present study. Using a micromanipulator (SM-191, Narishige, Tokyo, Japan), an epoxy-insulated tungsten microelectrode (impedance = 1–8 MΩ at 1 kHz; FHC, Bowdoinham, ME, USA) was initially inserted 0 ± 0.2 mm anterior or posterior to the boundary of the inferior colliculus and cerebellum, 1.3 ± 0.1 mm lateral to the midline while stimulating the oral cavity with a search stimulus (a mixture of 0.5 M sucrose, 0.3 M NaCl, 0.02 M citric acid, and 0.02 M QHCl). Most typically the electrode hit the gustatory zone 2.9 ± 0.2 mm ventral to the surface of the inferior colliculus. Neuronal activity was amplified and monitored with a computer-aided data-acquisition and analysis system (CED 1401, Spike2 version 4.01; Cambridge Electronic Design, Cambridge, UK).

After isolating a single unit in the PbN, taste stimuli were applied to the oral cavity at room temperature (23–24°C). The tongue was extended using a string glued to its ventral surface to make it easier to stimulate posterior taste buds innervated by the glossopharyngeal nerve. The oral cavity was stimulated with a method modified from our previous studies with rats (e.g. Shimura et al., 2002). Fluid stimuli were delivered through a length of intraorally inserted slender tubing (PE 100), with the end positioned approximately 2 mm above the dorsal anterior tongue. During stimulus delivery, fluid could be seen engaging both the tongue and palate, and preliminary experiments using methylene blue dye suggested that this method reliably bathes the entire oral cavity. Five milliliters of each taste stimulus was presented at a rate of 0.5 ml/s, delivered under mild pressure from a 5 ml syringe. Each stimulus trial consisted of a 10-s rinse of distilled water, 10-s stimulus, and 10-s rinse of distilled water, all presented at the same rate. Gustatory stimuli and water were cleared from the delivery tubing by air pressure. Stimulus onset could also be determined by a response artifact that occurred when the stimulus first contacts the tongue (e.g. Bradley and Mistretta, 1980). When taste-evoked neural activity persisted after the 10-s poststimulus rinse of

distilled water, we continued the water rinse until the activity returned to the prestimulus level. At least 90 seconds were allowed to elapse between stimuli to avoid the effects of adaptation. When possible, taste stimuli were presented more than 2 times each.

Data analysis

A neuron was considered to be taste-responsive if the neural activity evoked by at least one of taste stimuli increased or decreased ≥ 2 SD from the mean of its spontaneous activity. All data analyses were based on neural activity quantified in 10-s samples. Spontaneous activity and responses to prestimulus water were calculated from multiple samples. The spontaneous rate was determined during the 10-s period just before the prestimulus water rinse. Water and taste neural responses were calculated during the first 10-s period after the onset of stimulation with prestimulus water or a taste solution. The net response rate, obtained by subtracting the immediately preceding raw water responses from the raw taste responses, was used for data analyses. The averages of net responses were used when taste stimulation was repeated. Each neuron was classified into sucrose (S)-best, NaCl (N)-best, citric acid (C)-best or QHCl (Q)-best categories based on which of the prototypical taste stimuli (0.5 M sucrose, 0.1 M NaCl, 0.01 M citric acid, 0.01 M QHCl, and 0.1 M MPG) evoked the greatest net response (e.g. Frank, 1973). This classification by best stimulus was further explored with cluster analysis; for this analysis, we used the Pearson product–moment correlation coefficients between response profiles of the neurons, and the unweighted pair-group average method.

With the use of adjusted response data, the breadth-of-tuning of each cell was calculated to measure the range of taste response sensitivity according to the formula for entropy (Smith and Travers, 1979; Travers and Smith, 1979)

$$H = -K\left(\sum_{i=1}^{4} Pi \log Pi\right)$$

where *Pi* represents the proportional response to each of the 4 basic taste stimuli and *K* is a scaling constant (1.661 for 4 stimuli). Values of entropy (*H*) ranges from 0.0 to 1.0. The neurons responding to many of four basic taste stimuli have greater *H* values (broad tuning) whereas the neurons responding only to small numbers of tastes express smaller *H* values (narrow tuning). In the present study *H* was obtained using the excitatory components of responses to four basic taste stimuli. The response to MPG, a prototypical umami stimulus, was not considered in this calculation, both for consistency with other published reports, and due to the fact that this stimulus was overall ineffective in driving neuronal responses (see Results).

In addition to *H*, we also calculated a second measure of neuronal breadth of responsiveness: The noise-to-signal (N/S) ratio (Spector and Travers, 2005). This ratio is derived by dividing the response to the second best stimulus (the maximum noise elicited by sideband stimuli) by the response to the best stimulus (signal). Similar to *H*, this measure also ranges from 0.0 to 1.0.

We characterized all taste-responsive neurons as possessing an umami synergistic response or not by calculating the synergistic ratio via a formula: magnitude of response to mixture/sum of magnitudes of responses to individual components (0.1 M MPG and 0.01 M IMP) in the mixture. If the magnitude of response to mixture was negative, the synergistic ratio was judged as zero. In theory, a ratio greater than 1.0 would be classified as synergistic. However, it is possible for the ratio to slightly exceed (or fall under) 1.0 in cells with small magnitude non-synergistic responses. We therefore used the previously established criterion of 1.2 (Ninomiya and Funakoshi, 1989; Tokita et al., 2012; Tokita and Boughter, 2012).

Magnitude of response to all taste stimuli was compared with repeated measure analysis of variance (ANOVA) in neurons recorded from three different PbN subdivisions (medial, brachium conjunctivum [BC] and lateral) and from caudal or rostral levels. Mean responses were compared in neurons that possessed or did not possess synergistic responses to the MPG + IMP mixture (neuron type × stimulus). Mean *H* values and N/S ratio were also examined with respect to region and level using ANOVA. Post hoc comparisons were performed using a bonferroni correction. To examine the possibility of differential distribution of recording sites of each neuron type (classification based on best stimulus, *H* values or N/S ratio), Fisher's exact probability test was applied.

All statistical analyses described above were performed using a general statistics package (Statistica version 6, StatSoft, Tulsa, OK, USA). The statistical rejection criterion for all tests was set at $P < 0.05$.

Histology

An electrolytic lesion was made in the PbN by passing current (20 μA for 20 s, electrode positive) at the final recording site of a recording session to reconstruct all recording sites (Fig 1). Following this, mice were anesthetized with intraperitoneally injected 25% urethane (0.5 ml) and perfused transcardially with phosphate-buffered saline and 10% formalin. The brains were removed and placed in 10% formalin at 4°C for 24 hours and then transferred to a 30% buffered sucrose solution and stored at 4°C for at least 5 days. Serial coronal sections were prepared at 40 μm thick using a freezing microtome, and then stained with cresyl violet. The location of each recording site was histologically imaged and reconstructed by using a microscope (DMRXA2, Leica Microsystems, Bannockburn, IL, USA) equipped with a digital camera (Hamamatsu ORCA-ER, Hamamatsu Corp., Shizuoka, Japan) and imaging software (SimplePCI, Hamamatsu Corp., Shizuoka, Japan).

Mediolaterally, recording sites were classified into three subdivisions of the PbN; medial (consisting of medial, dorsal medial and external medial subnucleus), BC, and lateral subdivisions (consisting of central lateral, dorsal lateral, external lateral, internal lateral and ventral lateral subnucleus). Note that subnuclei belonging to the lateral subdivision lie dorsal to the BC, and all subnuclei except for the dorsal medial subnucleus belonging to the medial subdivision lie ventral to the BC. To avoid confusion, here we consistently use the terms "medial" and "lateral" to refer to the areas ventral and dorsal to the BC even when we cite articles which use these latter terms (e.g. Van Buskirk and Smith, 1981; Ogawa et al., 1987; Halsell and Travers, 1997; Shimura et al., 2002). Recording sites found in sections more

rostral or caudal than −180 μm to the caudal end of the cuneiform nucleus were classified as *rostral* (which correspond to recording sites plotted in panels A and B in Figs. 6, 8 and 9) and *caudal* PbN (which correspond to recording sites plotted in panels C and D in Figs. 6, 8 and 9), respectively.

Results

Basic characteristics

A total of 56 taste-responsive neurons were isolated and recorded from the PbN of 22 mice while all taste stimuli were presented. These data were combined with 122 neurons collected in our previous studies (Tokita et al., 2012; Tokita and Boughter, 2012), to comprise a total number of 178 individual recorded neurons. Therefore, the total number of individual neurons analyzed was 178 in the present study. All neurons showed excitatory activity to at least one of the 4 basic taste stimuli (sucrose, NaCl, citric acid, or QHCl). The mean spontaneous firing rate (spikes/s) of all neurons was 1.12 ± 0.12 (range: 0.0–10.14). The mean *H* and N/S ratio across all neurons were 0.64 ± 0.02 (range: 0.0–0.98) and 0.43 ± 0.02 (range: 0.0–0.98), respectively. A *t*-test revealed that the mean values of *H* and N/S ratio were significantly different ($P < 0.01$).

Based on their largest net response to the 4 standard taste stimuli, as well as to MPG, we classified PbN neurons as follows: 76 S-best (42.7%), 59 N-best (33.1%), 24 C-best (13.5%) and 19 Q-best (10.7%). No neuron responded best to MPG (or IMP). Neurons were also classified as synergistic (n = 90, 50.6%) or non-synergistic (n = 88, 49.4%). The mean spontaneous firing rate (spikes/sec) for S-, N-, C-, Q-best neurons was 0.74 ± 0.13 (range: 0.0–7.2), 1.42 ± 0.27 (range: 0.0–10.14), 1.44 ± 0.23 (range: 0.01– 4.09), and 1.29 ± 0.42 (range: 0.0–6.18), respectively. A one-way ANOVA revealed a significant main effect of neuron type [$F_{(3,174)} = 2.7$, $P < 0.05$]. Post hoc analyses of these data using Bonferroni tests showed that S-best neurons had a significantly lower spontaneous firing rate than did N-best neurons ($P < 0.05$).

H and N/S ratio were determined for each recorded neuron (Fig 2A and B). Both measure provide an estimate of breadth-of-tuning, but differ in significant ways, with N/S ratio more sensitive to the disparity in absolute size between optimal and sideband response. It is suggested that examining both measures is necessary to reveal a complete picture of tuning (Spector and Travers, 2005). For S-, N-, C-, Q-best neurons, *H* was 0.61 ± 0.02 (range: 0.21–0.94), 0.59 ± 0.03 (range: 0.0–0.96), 0.79 ± 0.02 (range: 0.57–0.95), and 0.69 ± 0.06 (range: 0.0–0.98), respectively. A one-way ANOVA revealed a significant main effect of neuron type [$F_{(3,174)} = 5.9$, $P < 0.01$]. Post hoc analyses of these data (Bonferroni) showed that *H* was significantly higher in C-best than in S- and N-best neurons ($P < 0.01$). The N/S ratios for S-, N-, C-, Q-best neurons were 0.36 ± 0.03 (range: 0.06–0.98), 0.41 ± 0.04 (range: 0.0–0.99), 0.64 ± 0.04 (range: 0.18–0.97), 0.47 ± 0.08 (range: 0.0–0.94). A one-way ANOVA revealed a significant main effect of neuron type [$F_{(3,174)} = 6.7$, $P < 0.01$]. Post hoc analyses (Bonferroni) showed that the N/S ratio was significantly higher in C-best than in S- and N-best neurons ($P < 0.01$). Figure 2C shows correlation between *H* and N/S ratio. Correlation coefficients for all neurons and each S-, N-, C-, Q- best neurons were 0.78, 0.73, 0.82, 0.65 and 0.75, respectively.

Taste response profiles and synergistic responses

Fig 3A displays the total gustatory net response profiles for all neurons to each of the 7 stimuli. Taste neurons were ordered by best-stimulus category, and within each category, by response magnitude. It is evident that among stimuli tested, sucrose and the umami mixture share a similar pattern of responses across all neurons. In fact, of the 90 neurons showing umami synergism, 76 were S-best neurons (100% of this type), and the remaining 14 were N-best neurons (23.7% of this type). Mean response rates of each type of neurons to taste stimuli are shown in Fig 3B. The veracity of our best-stimulus classification was further explored using cluster analysis based on the responses of each neuron to all stimuli (Fig 3C). The analysis identified 4 major clusters consisting of cells highly responsive to sucrose, NaCl, citric acid and QHCl (S, N, C and Q clusters). Of 178 neurons, only 12 grouped with a cluster different from the best response; half of these were N-best cells in the C cluster. The majority of cells in the S cluster and some of the cells in the N clusters showed umami synergism whereas no such cells were found in the C and Q clusters.

Synergistic ratios for each neuron classified as synergistic (gray circle) and non-synergistic (open circle) are shown in Fig 4. The criterion 1.2 (Ninomiya and Funakoshi 1989; Tokita et al., 2012; Tokita and Boughter 2012) corresponds to a natural breakpoint in the data, with 21 of 88 non-synergistic cells possessing ratios greater than 1 but less than 1.14; the first clearly synergistic neuron possessed a ratio of 1.36. Synergistic responses were typically (but not in all cases) confirmed with multiple trials with 0.1M MPG, 0.01 M IMP, and their mixture. Mean net taste responses (±SEM) to taste stimuli in synergistic and non-synergistic neurons are shown in Fig 5A – C. A two-way ANOVA with repeated measures (neuron type × stimulus) was applied to taste responses of all synergistic (n = 90) and non-synergistic neurons (n = 88) (Fig 5A). This analysis revealed significant main effect of neuron type [$F_{(1,176)} = 23.5$, $P < 0.01$] and stimulus [$F_{(7,1232)} = 107.6$, $P < 0.01$], as well as a significant neuron type × stimulus interaction [$F_{(7,1232)} = 122.1$, $P < 0.01$]. Post hoc tests (Bonferroni) showed that whereas synergistic neurons responded more strongly to sucrose and the MPG + IMP mixture, non-synergistic neurons responded more strongly to citric acid and QHCl ($P < 0.01$). Further analysis of synergistic vs. non-synergistic neurons within best-stimulus groups revealed that these preferential responses differed in S-best vs. N-best cells (Fig 5B and C). In S-best cells, there was a significant main effect of neuron type [$F_{(1,162)} = 20.8$, $P < 0.01$] and stimulus [$F_{(7,1134)} = 115.7$, $P < 0.01$], and a significant neuron type × stimulus interaction [$F_{(7,1134)} = 156.6$, $P < 0.01$]. Synergistic neurons responded more robustly to sucrose and the mixture, and less robustly to NaCl, citric acid, QHCl ($P < 0.01$). In N-best cells, there was a significant main effect of neuron type [$F_{(1,57)} = 9.1$, $P < 0.01$] and stimulus [$F_{(7,399)} = 71.9$, $P < 0.01$]. The neuron type × stimulus interaction was also significant [$F_{(7,399)} = 11.7$, $P < 0.01$]. Synergistic N-best cells responded more strongly than the non-synergistic cells to sucrose, the mixture and NaCl ($P < 0.05$ for NaCl; $P < 0.01$ for sucrose and MPG + IMP mixture), but did not differ for the other stimuli.

Histology

Based on stereotaxic coordinates of recording sites and the marking lesions made in the final recording sites (e.g. Fig 1), the locations of all 178 taste-responsive PbN neurons were successfully reconstructed. Neuronal location was plotted according to best stimulus in

rostrocaudally arranged PbN schema at 4 different levels (Fig 6A – D). Recording sites were located in the medial, central lateral, ventral lateral, and external lateral subnuclei as well as in the BC. No gustatory neurons were isolated in other areas such as dorsal medial, external medial, dorsal lateral or internal lateral subnuclei.

The mediolateral distribution of recording sites in terms of neuron type (based on best stimulus) is summarized in Table 1. Recording sites were classified into medial (medial subnucleus), BC, and lateral subdivisions (central lateral, ventral lateral and external lateral subnuclei). Fisher's exact probability test revealed that the proportion of neuron types in the medial vs. lateral and BC vs. lateral subdivisions was significantly different, with a greater amount of S-best neurons found medially ($P < 0.01$) and within the BC ($P < 0.01$). There was no difference in neuron type distribution between the medial and BC subdivisions. We also examined the rostrocaudal distribution of recording sites in terms of neuron type based on best stimulus (Table 2). Neurons in the rostral and caudal PbN correspond to those plotted in panels A–B and C–D of Fig 6, respectively. Fisher's exact probability test revealed no significant difference in the rostrocaudal distribution of each neuron type ($P = 0.08$).

Mean net responses to taste stimuli, and mean spontaneous activity, were next compared in PbN neurons (Fig 7) with respect to region (medial, BC and lateral subdivisions) and level (rostral vs. caudal). A three-way ANOVA (stimulus × region × level) indicated a significant main effect of stimulus [$F_{(7,469)} = 59.85$, $P < 0.0001$], but not region or level. Additionally, there was a significant stimulus × region interaction [$F_{(14,469)} = 6.93$, $P < 0.0001$], which was further explored via a two-way ANOVA with post-hoc comparisons (Fig 7A). Responses to sucrose and the MPG + IMP mixture of neurons in the medial and BC subdivisions were significantly greater than those of neurons in the lateral subdivision ($P <$ 0.01 and 0.05, respectively). On the other hand, neurons in the lateral and BC subdivisions showed significantly greater responses to QHCl than neurons in the medial subdivision ($P <$ 0.01 and 0.05, respectively). In the three-way ANOVA, the stimulus × level, and region × level interactions were not significant (Ps > 0.3); mean net responses to taste stimuli and spontaneous firing rate of neurons in the rostral and caudal PbN did not appear to differ (Fig 7B). However, a small but significant stimulus × level × region interaction [$F_{(14,469)} = 1.85$, $P < 0.04$] suggested that the differences shown in Fig 7A may be dependent to some degree on level.

We also examined neuron location with respect to *H* and N/S ratio (Figs. 8 and 9). Neurons were classified into 1 of 5 categories of each value (Tables 3 and 4). Fisher's exact probability test revealed that the proportion of neurons in the medial vs. lateral subdivision was significantly different, with a greater amount of neurons possessing high *H* (i.e. more broadly tuned) found laterally ($P < 0.05$) whereas the proportion of neurons in medial vs. BC and BC vs. lateral subdivisions did not differ ($P = 0.19$ and 0.78, respectively). However, two-way ANOVA (region × level) revealed no significant main effect of region on mean *H*. Overall, this value was similar among neurons recorded in medial (0.58 ± 0.03, range: 0.0–0.91), BC (0.66 ± 0.03, range: 0.08–0.98), and lateral (0.66 ± 0.03, range: 0.0–0.95) subdivisions (Fig 10A). In contrast to *H*, there was no significant difference in the mediolateral distribution of neurons in terms of N/S ratio (Fisher's exact probability test,

Table 4) and mean N/S ratio (two-way ANOVA, region × level, no significant main effects or interaction) (Fig 10B).

Analyses on rostral vs. caudal levels were also performed using *H* and N/S ratio as measures (e.g. Figs. 8, 9 and 10, and Tables 5 and 6). Fisher's exact probability test revealed that the proportion of neurons classified according to *H* did not differ significantly between levels ($P = 0.14$, Table 5). However, results from the two-way ANOVA (region × level) revealed a significant main effect of level [$F_{(1,172)} = 4.3$, $P < 0.04$]. Mean *H* values were higher in the caudal (0.67 ± 0.02, range: 0.0–0.98, data from panels Fig 8C and D) than in the rostral PbN (0.59 ± 0.03, range: 0.0–0.96, data from panels Fig 8A and B, $P < 0.05$) (Fig 10A). Again, there was no significant difference in the rostrocaudal distribution of neurons in terms of N/S ratio (Fisher's exact probability test, Table 6) and mean N/S ratio (ANOVA discussed above) (Fig 10B). Among individual neurons, *H* and N/S ratio were closely related, whether within mediolateral subdivisions or rostral vs. caudal levels. The correlation coefficients for medial, BC, lateral, rostral and caudal subdivisions were 0.80, 0.73, 0.79, 0.79 and 0.76, respectively (Fig 10C).

Discussion

Taste response profiles and umami responses

In the present study, S-best (n = 76, 42.7 %) and N-best neurons (n = 59, 33.1 %) comprised about 76 % of the data, followed by C-best (n = 24, 13.5 %) and Q-best neurons (n = 19, 10.7 %). This distribution of neuron type is generally consistent with data from the taste-responsive neurons in the NST of C57BL/6J mice (McCaughey, 2007; Lemon and Margolskee, 2009; Wilson and Lemon, 2014). Compared to previous studies in the rat PbN, the present data is characterized by a greater number of S-best neurons and less N-best neurons (Spector and Travers, 2005). The abundant number of S-best neurons in the PbN may contribute to the physiological bases for high behavioral avidity to sweetness in C57BL/6J mice relative to some other strains (e.g. Boughter and Bachmanov, 2007), as it does in the NST (McCaughey, 2007).

No neuron responded best to the umami stimulus MPG or IMP presented alone (Fig 2). The lack of neurons responsive best to umami stimuli contrasts sharply to the previous finding that mouse chorda tympani and glossopharyngeal nerves contain MSG-or MPG-best single fibers (Ninomiya and Funakoshi, 1989; Yasumatsu et al., 2012). Several factors must be considered in the weak response to these stimuli in our study. As it is highly unlikely that we failed to stimulate the anterior tongue (innervated by chorda tympani), this discrepancy may reflect the different information processing or neural coding strategy of umami taste in the periphery vs. brain. In fact, physiological and anatomical studies in rodents indicate that inputs from the chorda tympani and glossopharyngeal nerves converge at the level of the NST, which likely differentiates central gustatory responsiveness from that in the periphery, and may account for the present discrepancy (Travers et al., 1986; Sweazey and Smith, 1987; Travers and Norgren, 1995; Grabauskas and Bradley, 1996; Corson and Erisir, 2013). Another possibility, however, is that we failed to optimally stimulate the posterior tongue. Although preliminary experiments suggested adequate bathing of the oral cavity, stimulation

of posterior taste buds depends on stimuli diffusing into the trenches of the vallate and foliate papillae.

Interestingly, recent behavioral evidence suggests that glutamate-salt compounds may be only weakly effective taste stimuli in mice, and that effectiveness may depend on the cation. Smith and Spector (2014) showed that mice could not detect MSG in a taste discrimination task once amiloride was added (to block the transduction of sodium). Saites et al. (2015) were unable to condition a taste aversion to MPG in mice, even when a high concentration (1.0 M) was used as the conditioned stimulus. The response to 0.01 M IMP in S-best cells was slightly stronger than that to 0.1 M MPG in the current study; interestingly, wild-type mice could detect IMP in the Smith and Spector (2014) study.

According to the present data, synergistic responses to a glutamate-5'-nucleotide mixture (Kurihara, 2015), one of the striking characteristics of umami taste, is represented almost entirely by S- and N-best neurons in the mouse PbN (Figs. 3, 4 and 5). In an earlier study, synergistic mixtures also preferentially activated sucrose-sensitive neurons in the PbN of awake rats (Nishijo et al., 1991), showing that anesthesia does not preclude this association. The finding that all 76 S-best and 14 sucrose-sensitive N-best neurons possessed synergistic responses is very consistent with and may at least in part explain behavioral data that mice show cross-generalization of conditioned taste aversion between sucrose and MPG + IMP mixture, i.e. mice likely perceive synergistic umami mixtures as tasting sweet (Saites et al., 2015). Despite activating different T1R receptor heterodimers in taste cells (e.g. Zhao et al., 2003; Zhang et al., 2008; Smith and Spector, 2014), both the neural and behavioral similarity between sucrose and the mixture, and the concomitant weakness of the glutamate-only response, raise questions about the salience or importance of a distinct "umami" taste in mice. As these qualities are clearly distinguishable in humans (Yamaguchi, 1991), it is reasonable to assume that a species difference exists, which may reflect a species-specific dietary strategy (e.g. Glendinning, 1994; Breslin, 2013).

Breadth of responsiveness measured by *H* and N/S ratio

In the present study, breadth of responsiveness was assessed by 2 different measures, *H* and N/S ratio. N/S ratio is a novel measure suggested by Spector and Travers (2005) whereas *H* has long been used in taste research (Smith and Travers, 1979; Travers and Smith, 1979). Although *H* and N/S ratio were positively correlated both in terms of neuron type and recording site (Figs. 2C and 10C), the distribution pattern of these two values were quite different (modes for *H* and N/S ratio were 0.85–0.90 and 0.15–0.20, respectively) (Fig 2A and B) and the mean *H* value of all neurons (0.64) was significantly higher than that of N/S ratio (0.43). In other words, when the maximum sideband noise (i.e. responses to the second best stimulus) is taken into account, the tuning of gustatory PbN neurons appears to be much narrower than estimated by *H*, a conclusion at least qualitatively consistent with the distribution of responses shown in Fig. 3. In terms of topographic organization, we detected some tuning-dependent topography in the PbN using *H* but not N/S ratio (Figs. 8–10 and Tables 3–6); the more salient topography involves best-quality response, rather than breadth-of-responsiveness.

Mediolateral differences in taste responsivity in the mouse PbN

Recording sites in the PbN were distributed in the medial and lateral subdivisions of the PbN, and also within the BC (Fig 6 and Table 1). In terms of subnuclei (Hashimoto et al., 2009; Tokita et al., 2010), recordings were made in the medial, central lateral, ventral lateral, and external lateral subnuclei but not in the dorsal medial, external medial, internal lateral, and dorsal lateral subnuclei regardless of penetrations into these areas in some animals.

Some previous *in vivo* extracellular electrophysiological studies in rodents suggested the existence of mediolateral topography in the taste-responsive area of the PbN. Van Buskirk and Smith (1981) showed that N-best neurons are preferentially located in the medial subdivision, hydrochloric acid-best neurons in the lateral subdivision, and S-best neurons equally in the medial and lateral subdivisions in the hamster. Ogawa et al. (1987) reported that N-best neurons were frequently found in the medial subdivision and hydrochloric acid-best neurons in the lateral subdivision in the rat. This distribution patterns were generally supported in other studies (Halsell and Travers, 1997; Shimura et al., 2002). In our study, acid-best (C-best) neurons were also found preferentially in the lateral subdivision. However, the medial-BC dominance of S-best neurons, and lateral dominance of N- and Q-best neurons has not been reported previously in other rodent species. Interestingly, the mediolateral distribution of neurons responding best to the most appetitive stimulus sucrose and to the most aversive stimulus QHCl seems to be a mirror image (Table 1). This mirror-image pattern was also observed in mean magnitude of response of all neurons in these 2 subdivisions to sucrose and QHCl (Fig 7A). Furthermore, medial-lateral differences were also evident in the distribution pattern of neuron type classified by *H* value (Fig 8 and Table 3), although mean *H* values across the mediolateral axis were not significantly different (Fig 10A). Collectively, these results suggest that both a sweet-bitter and a narrow-broad tuning gradient is roughly represented along a mediolateral axis in the mouse PbN. Functionally, these gradients might reflect patterns of convergence, or differential projections of PbN neurons to forebrain targets. For example, more cells projecting to taste thalamus (parvicellular part of the ventroposteromedial nucleus of the thalamus) than to the central nucleus of the amygdala or lateral hypothalamus are found medially and in the BC (Tokita et al., 2010). Laterally, projections are more varied.

Rostrocaudal differences in taste responsivity in the mouse PbN

More taste-responsive neurons were recorded in the caudal than in the rostral PbN in the present study (103 vs. 75). This caudal dominance of taste responsiveness in the PbN is consistent with previous studies in the rat and hamster (Halsell and Frank, 1991; Halsell and Travers, 1997). However, the present data are not consistent with previous rat and hamster studies reporting that N-best neurons are most frequently found caudally (Van Buskirk and Smith, 1981; Ogawa et al., 1987; Halsell and Travers, 1997) and acid-sensitive neurons (hydrochloric acid-best neurons) rostrally (Van Buskirk and Smith, 1981; Ogawa et al., 1987). This discrepancy may be due to a species difference, including the fact that the mouse PbN is anatomically smaller and more compact than that of the rat or hamster. Although the distribution of neuron type based on best stimulus and *H* value (Figs. 6 and 8, Tables 2 and 5) and response magnitude to all taste stimuli (Fig 7B) were not significantly

different along the rostrocaudal axis, the mean *H* in the caudal PbN was significantly higher than that in the rostral PbN (Fig 10A). The abundant input from the rostral gustatory NST to the caudal PbN of rodents including mice (Herbert et al., 1990; Whitehead et al., 2000; Karimnamazi et al., 2002; Zaidi et al., 2007; Ganchrow et al., 2014) may contribute to the broadly tuned responsiveness in this subdivision (i.e. possibility of more convergence). This finding is also commensurate with the fact that significantly more NST-PbN projection neurons are known to respond to three or more basic taste stimuli than non-projection neurons in the rat (Monroe and Di Lorenzo, 1995).

Comparison to findings from c-Fos immunohistochemistry

Some PbN subnuclei are known to differentially express robust c-Fos depending on the taste stimulus applied to the oral cavity; for example, sucrose preferentially evokes c-Fos in the dorsal lateral subnuclus (Yamamoto, 1994; Sawa and Yamamoto, 2000; Tokita et al., 2014), NaCl in the dorsal lateral subnuclus and medial subnucleus (Yamamoto, 1994; Tokita et al., 2007; Hashimoto et al., 2009; Tokita et al., 2014), and hydrochloric acid and QHCl in the external lateral and external medial subnuclei (Yamamoto et al., 1994; Travers et al., 1999; King et al., 2003; Tokita et al., 2014). QHCl also induces c-Fos in the dorsal medial subnucleus in mice (Tokita et al., 2014). Among these subnuclei, the dorsal medial and dorsal lateral subnuclei have not been typically regarded as taste-responsive in single-unit electrophysiological studies (e.g. Halsell and Travers, 1997; Geran and Travers, 2009). We failed to record taste responses from these areas, in addition to the external medial subnucleus, where just a small number of neurons were found to be electrophysiologically taste-responsive in the rat (Halsell and Travers, 1997).

These discrepancies between c-Fos and physiological studies may be merely due to the difficulty in electrophysiological single-unit isolation because of small-sized or densely packed cell bodies in these subnuclei. However, Halsell and Frank (1991), who made careful multi- but not single-unit maps in the hamster PbN, also did not report taste activity in the same subnuclei where we failed to do so, i.e. dorsal lateral, dorsal medial, and external medial subnuclei. It is possible that taste-evoked c-Fos expression in these regions may reflect post-ingestive signaling or other factors rather than purely sensory taste stimulation. This interpretation is supported by a previous study by King et al. (2003), who showed that bilateral transection of the glossopharyngeal nerve caused a significant decrease in quinine-evoked c-Fos in the waist area, but not external medial or external lateral subnuclei. An additional methodological consideration is that c-Fos expression is evoked by taste stimulation in an awake mouse, whereas our single-cell recordings were made in anesthetized mice. Recent awake recordings in the PbN of rats demonstrate an additional complexity to taste responses, including neurons whose firing is modulated by licking (Weiss et al., 2014).

Topographic organization in the taste CNS

Traditionally, both electrophysiological and c-Fos studies of the central gustatory system have described substantial overlap in terms of both quality representation and breadth of tuning, as opposed to a strict segregation (e.g. Van Buskirk and Smith, 1981; Yamamoto et al., 1985; Ogawa et al., 1987; Yamamoto et al., 1994; Harrer and Travers, 1996; Katz et al.,

2001; Stratford and Finger, 2011; Yokota et al., 2014). The current study is consistent with others in suggesting that a significant degree of taste quality organization exists within this heterogeneous framework. This type of topography, which has also been referred to as "chemotopy" (Travers, 1993) or "gustotopy" (Chen et al., 2011), has been most extensively investigated in the NST, the first-order brain taste center. In line with previous rat studies (Harrer and Travers, 1996; Travers, 2002), QHCl stimulation evoked c-Fos expression in the medial third of the rostral part of the nucleus in inbred and transgenic mice (Travers et al., 2007). Recently, NaCl and MSG have also been shown to elicit distinctive c-Fos expression in this nucleus in wild type mice (Stratford and Finger, 2011). In the hamster, salient multi-unit responses to NaCl were found rostral to regions where sucrose and potassium chloride evoked the strongest response in the taste-responsive area of the NST (McPeeters et al., 1990), which is generally consistent with findings from a recent single-unit study in the rat (Yokota et al., 2014). In terms of oro-spatial organization, gustatory neurons responsive to anterior oral cavity stimulation are located anterior to those responsive to posterior oral cavity stimulation in the rat (Travers and Norgren, 1995; Geran and Travers, 2006). Collectively, topographic organization in the first central taste relay NST appears to exist and have some functional significance (Yokota et al., 2014). It is therefore highly likely that this organization is preserved in higher taste relays including the PbN.

Aside from NST and PbN, the other taste area that has been studied with regards to topography is the gustatory cortex, located within insular cortex. Physiological recordings from rats indicate that cortical neurons tend to be heterogeneous in terms of quality coding and breadth-of-responsiveness (e.g. Ogawa et al., 1992; Hanamori et al., 1998; Simon et al., 2006), and similar to the brainstem areas there is some tendency for segregation of primary tastes, including sucrose responses anterodorsally and quinine responses posteriorly (Yamamoto et al., 1985). This latter result was supported by an *in vivo* surface optical imaging study that reported distinct, yet substantially overlapping activation patterns in response to basic tastes in the rat (Accolla et al., 2007). However, these findings were challenged by a recent *in vivo* two-photon calcium imaging study in mice showing gustatory cortex appears to have densely-packed, mutually separated neuronal cell groups selectively tuned for only one taste quality (Chen et al., 2011). Indeed, optogenetic and pharmacological manipulations in the disparate sweet and bitter cortical fields delineated in the latter study appeared to elicit corresponding gustatory perceptual consequences (Peng et al., 2015). The discovery of this apparent strict chemotopy draws a sharp contrast to findings of the present study as well as previous studies in other rodent species than mice. Interestingly, a recent high-resolution lesion-mapping study in the rat gustatory cortex revealed the existence of a specific "hot spot" involved in conditioned taste aversion (Schier et al., 2014), suggesting that topographical organization is shaped by function.

Conclusion

In summary, the present study shows that the mouse PbN possesses topographical organization in terms of the distribution of primary taste qualities (each best-neuron type), as well as response magnitude and breadth of tuning (entropy, *H*). These findings were made using a relatively large database of 178 characterized taste-responsive neurons. These findings confirm and expand on our earlier analyses, and are consistent with the majority of

previous studies that demonstrate organization in multiple areas of the taste CNS according to primary tastes. Importantly, this organization appears to exist along a spatial gradient rather than take the form of absolute segregation of tastes.

Acknowledgements

The authors thank Drs. Matthew Ennis for technical support and Steven St. John for valuable comments. Funding for this research was received from NIH grant DC000353 and the Ajinomoto Amino Acid Research Program to J. D. Boughter, Jr.

References

Accolla R, Bathellier B, Petersen CC, Carleton A. Differential spatial representation of taste modalities in the rat gustatory cortex. J Neurosci. 2007; 27:1396–1404. [PubMed: 17287514]

Boughter JD Jr, Bachmanov AA. Behavioral genetics and taste. BMC Neurosci. 2007; 8(Suppl 3):S3. [PubMed: 17903279]

Bradley RM, Mistretta CM. Developmental changes in neurophysiological taste responses from the medulla in sheep. Brain Res. 1980; 191:21–34. [PubMed: 7378752]

Breslin PA. An evolutionary perspective on food and human taste. Curr Biol 2013. 2013; 23:R409–R418.

Butler, A.; Hodos, W. Comparative vertebrate neuroanatomy. New York, NY: Wiley-Liss; 1996.

Carter ME, Han S, Palmiter RD. Parabrachial calcitonin gene-related peptide neurons mediate conditioned taste aversion. J Neurosci. 2015; 35:4582–4586. [PubMed: 25788675]

Chandrashekar J, Hoon MA, Ryba NJ, Zuker CS. The receptors and cells for mammalian taste. Nature. 2006; 444:288–294. [PubMed: 17108952]

Chaudhari N, Roper SD. The cell biology of taste. J Cell Biol. 2010; 190:285–296. [PubMed: 20696704]

Chen X, Gabitto M, Peng Y, Ryba NJ, Zuker CS. A gustotopic map of taste qualities in the mammalian brain. Science. 2011; 333:1262–1266. [PubMed: 21885776]

Corson JA, Erisir A. Monosynaptic convergence of chorda tympani and glossopharyngeal afferents onto ascending relay neurons in the nucleus of the solitary tract: a high-resolution confocal and correlative electron microscopy approach. J Comp Neurol. 2013; 521:2907–2926. [PubMed: 23640852]

Dickman JD, Smith DV. Topographic distribution of taste responsiveness in the hamster medulla. Chem Senses. 1989; 14:231–247.

Frank M. An analysis of hamster afferent taste nerve response functions. J Gen Physiol. 1973; 61:588–618. [PubMed: 4705639]

Ganchrow D, Ganchrow JR, Cicchini V, Bartel DL, Kaufman D, Girard D, Whitehead MC. Nucleus of the solitary tract in the C57BL/6J mouse: Subnuclear parcellation, chorda tympani nerve projections, and brainstem connections. J Comp Neurol. 2014; 522:1565–1596. [PubMed: 24151133]

Geran LC, Travers SP. Single neurons in the nucleus of the solitary tract respond selectively to bitter taste stimuli. J Neurophysiol. 2006; 96:2513–2527. [PubMed: 16899635]

Geran LC, Travers SP. Bitter-responsive gustatory neurons in the rat parabrachial nucleus. J Neurophysiol. 2009; 101:1598–1612. [PubMed: 19129294]

Glendinning JI. Is the bitter rejection response always adaptive? Physiol Behav. 1994; 56:1217–1227. [PubMed: 7878094]

Grabauskas G, Bradley RM. Synaptic interactions due to convergent input from gustatory afferent fibers in the rostral nucleus of the solitary tract. J Neurophysiol. 1996; 76:2919–2927. [PubMed: 8930244]

Halpern BP, Nelson LM. Bulbar gustatory responses to anterior and to posterior tongue stimulation in the rat. Am J Physiol. 1965; 209:105–110. [PubMed: 14343744]

Halsell CB, Frank ME. Mapping study of the parabrachial taste-responsive area for the anterior tongue in the golden hamster. J Comp Neurol. 1991; 306:708–722. [PubMed: 2071702]

Halsell CB, Travers SP. Anterior and posterior oral cavity responsive neurons are differentially distributed among parabrachial subnuclei in rat. J Neurophysiol. 1997; 78:920–938. [PubMed: 9307125]

Hanamori T, Kunitake T, Kato K, Kannan H. Responses of neurons in the insular cortex to gustatory, visceral, and nociceptive stimuli in rats. J Neurophysiol. 1998; 79:2535–2545. [PubMed: 9582226]

Harrer MI, Travers SP. Topographic organization of Fos-like immunoreactivity in the rostral nucleus of the solitary tract evoked by gustatory stimulation with sucrose and quinine. Brain Res. 1996; 711:125–137. [PubMed: 8680855]

Hashimoto K, Obata K, Ogawa H. Characterization of parabrachial subnuclei in mice with regard to salt tastants: possible independence of taste relay from visceral processing. Chem Senses. 2009; 34:253–267. [PubMed: 19179538]

Herbert H, Moga MM, Saper CB. Connections of the parabrachial nucleus with the nucleus of the solitary tract and the medullary reticular formation in the rat. J Comp Neurol. 1990; 293:540–580. [PubMed: 1691748]

Kaas JH. Topographic maps are fundamental to sensory processing. Brain Res Bull. 1997; 44:107–112. [PubMed: 9292198]

Karimnamazi H, Travers SP, Travers JB. Oral and gastric input to the parabrachial nucleus of the rat. Brain Res. 2002; 957:193–206. [PubMed: 12445962]

Katz DB, Simon SA, Nicolelis MA. Dynamic and multimodal responses of gustatory cortical neurons in awake rats. J Neurosci. 2001; 21:4478–4489. [PubMed: 11404435]

King CT, Deyrup LD, Dodson SE, Galvin KE, Garcea M, Spector AC. Effects of gustatory nerve transection and regeneration on quinine-stimulated Fos-like immunoreactivity in the parabrachial nucleus of the rat. J Comp Neurol. 2003; 465:296–308. [PubMed: 12949788]

Kurihara K. Umami the fifth basic taste: History of studies on receptor mechanisms and role as a food flavor. Biomed Res Int. 2015; 2015:189402. [PubMed: 26247011]

Lemon CH, Margolskee RF. Contribution of the T1r3 taste receptor to the response properties of central gustatory neurons. J Neurophysiol. 2009; 101:2459–2471. [PubMed: 19279151]

Lundy, RF., Jr; Norgren, R. Gustatory system. In: Paxinos, G., editor. The rat nervous system. 4th. San Diego, CA: Elsevier Academic Press; 2015. p. 733-760.

Magableh A, Lundy R. Somatostatin and corticotrophin releasing hormone cell types are a major source of descending input from the forebrain to the parabrachial nucleus in mice. Chem Senses. 2014; 39:673–682. [PubMed: 25086873]

McCaughey SA. Taste-evoked responses to sweeteners in the nucleus of the solitary tract differ between C57BL/6ByJ and 129P3/J mice. J Neurosci. 2007; 27:35–45. [PubMed: 17202470]

McPheeters M, Hettinger TP, Nuding SC, Savoy LD, Whitehead MC, Frank ME. Taste-responsive neurons and their locations in the solitary nucleus of the hamster. Neuroscience. 1990; 34:745–758. [PubMed: 2352650]

Monroe S, Di Lorenzo PM. Taste responses in neurons in the nucleus of the solitary tract that do and do not project to the parabrachial pons. J Neurophysiol. 1995; 74:249–257. [PubMed: 7472328]

Mori K, Takahashi YK, Igarashi KM, Yamaguchi M. Maps of odorant molecular features in the Mammalian olfactory bulb. Physiol Rev. 2006; 86:409–433. [PubMed: 16601265]

Ninomiya Y, Funakoshi M. Peripheral neural basis for behavioural discrimination between glutamate and the four basic taste substances in mice. Comp Biochem Physiol A Comp Physiol. 1989; 92:371–376. [PubMed: 2565788]

Nishijo H, Ono T, Norgren R. Parabrachial gustatory neural responses to monosodium glutamate ingested by awake rats. Physiol. Behav. 1991; 49:965–971.

Ogawa H, Hasegawa K, Murayama N. Difference in taste quality coding between two cortical taste areas, granular and dysgranular insular areas, in rats. Exp Brain Res. 1992; 91:415–424. [PubMed: 1483516]

Ogawa H, Hayama T, Ito S. Response properties of the parabrachio-thalamic taste and mechanoreceptive neurons in rats. Exp Brain Res. 1987; 68:449–457. [PubMed: 3691718]

Peng Y, Gillis-Smith S, Jin H, Tränkner D, Ryba NJ, Zuker CS. Sweet and bitter taste in the brain of awake behaving animals. Nature. 2015; 527:512–515. [PubMed: 26580015]

Saites LN, Goldsmith Z, Densky J, Guedes VA, Boughter JD Jr. Mice perceive synergistic umami mixtures as tasting sweet. Chem Senses. 2015; 40:295–303. [PubMed: 25820205]

Sako N, Tokita K, Sugimura T, Yamamoto T. Synergistic responses of the chorda tympani to mixtures of umami and sweet substances in rats. Chem Senses. 2003; 28:261–266. [PubMed: 12714449]

Schier LA, Hashimoto K, Bales MB, Blonde GD, Spector AC. High-resolution lesion-mapping strategy links a hot spot in rat insular cortex with impaired expression of taste aversion learning. Proc Natl Acad Sci U S A. 2014; 111:1162–1167. [PubMed: 24395785]

Shimura T, Tokita K, Yamamoto T. Parabrachial unit activities after the acquisition of conditioned taste aversion to a non-preferred HCl solution in rats. Chem Senses. 2002; 27:153–158. [PubMed: 11839613]

Simon SA, de Araujo IE, Gutierrez R, Nicolelis MA. The neural mechanisms of gustation: a distributed processing code. Nat Rev Neurosci. 2006; 7:890–901. [PubMed: 17053812]

Smith DV, Travers JB. A metric for the breadth of tuning of gustatory neurons. Chem Senses Flav. 1979; 4:215–229.

Smith KR, Spector AC. The importance of the presence of a 5'-ribonucleotide and the contribution of the T1R1 + T1R3 heterodimer and an additional low-affinity receptor in the taste detection of L-glutamate as assessed psychophysically. J Neurosci. 2014; 34:13234–13245. [PubMed: 25253867]

Spector AC, Travers SP. The representation of taste quality in the mammalian nervous system. Behav Cogn Neurosci Rev. 2005; 4:143–191. [PubMed: 16510892]

Stratford JM, Finger TE. Central representation of postingestive chemosensory cues in mice that lack the ability to taste. J Neurosci. 2011; 31:9101–9110. [PubMed: 21697361]

Sugita M, Shiba Y. Genetic tracing shows segregation of taste neuronal circuitries for bitter and sweet. Science. 2005; 309:781–785. [PubMed: 16051799]

Sweazey RD, Smith DV. Convergence onto hamster medullary taste neurons. Brain Res. 1987; 408:173–184. [PubMed: 3297247]

Thivierge JP, Marcus GF. The topographic brain: from neural connectivity to cognition. Trends Neurosci. 2007; 30:251–259. [PubMed: 17462748]

Tokita K, Armstrong WE, St John SJ, Boughter JD Jr. Activation of lateral hypothalamus-projecting parabrachial neurons by intraorally delivered gustatory stimuli. Front Neural Circuits. 2014; 8:86. [PubMed: 25120438]

Tokita K, Boughter JD Jr. Sweet-bitter and umami-bitter taste interactions in single parabrachial neurons in C57BL/6J mice. J Neurophysiol. 2012; 108:2179–2190. [PubMed: 22832571]

Tokita K, Inoue T, Boughter JD Jr. Afferent connections of the parabrachial nucleus in C57BL/6J mice. Neuroscience. 2009; 161:475–488. [PubMed: 19327389]

Tokita K, Inoue T, Boughter JD Jr. Subnuclear organization of parabrachial efferents to the thalamus, amygdala and lateral hypothalamus in C57BL/6J mice: a quantitative retrograde double labeling study. Neuroscience. 2010; 171:351–365. [PubMed: 20832453]

Tokita K, Shimura T, Nakamura S, Inoue T, Yamamoto T. Involvement of forebrain in parabrachial neuronal activation induced by aversively conditioned taste stimuli in the rat. Brain Res. 2007; 1141:188–196. [PubMed: 17276421]

Tokita K, Yamamoto T, Boughter JD Jr. Gustatory neural responses to umami stimuli in the parabrachial nucleus of C57BL/6J mice. J Neurophysiol. 2012; 107:1545–1555. [PubMed: 22170968]

Travers JB, Herman K, Yoo J, Travers SP. Taste reactivity and Fos expression in GAD1-EGFP transgenic mice. Chem Senses. 2007; 32:129–137. [PubMed: 17082515]

Travers JB, Smith DV. Gustatory sensitivities in neurons of the hamster nucleus tractus solitarius. Sens Processes. 1979; 3:1–26. [PubMed: 229568]

Travers JB, Urbanek K, Grill HJ. Fos-like immunoreactivity in the brain stem following oral quinine stimulation in decerebrate rats. Am J Physiol Regul Integr Comp Physiol. 1999; 277:R384–R394.

Travers, SP. Orosensory processing in neural systems of the nucleus of the solitary tract. In: Simon, SA.; Roper, SD., editors. Mechanisms of Taste Transduction. Boca Raton, FL: CRC Press; 1993. p. 339-394.

Travers SP. Quinine and citric acid elicit distinctive Fos-like immunoreactivity in the rat nucleus of the solitary tract. Am J Physiol Regul Integr Comp Physiol. 2002; 282:R1798–R1810. [PubMed: 12010763]

Travers SP, Norgren R. Organization of orosensory responses in the nucleus of the solitary tract of rat. J Neurophysiol. 1995; 73:2144–2162. [PubMed: 7666129]

Travers SP, Pfaffmann C, Norgren R. Convergence of lingual and palatal gustatory neural activity in the nucleus of the solitary tract. Brain Res. 1986; 365:305–320. [PubMed: 3947995]

Van Buskirk RL, Smith DV. Taste sensitivity of hamster parabrachial pontine neurons. J Neurophysiol. 1981; 45:144–171. [PubMed: 7205341]

Weiss MS, Victor JD, Di Lorenzo PM. Taste coding in the parabrachial nucleus of the pons in awake, freely licking rats and comparison with the nucleus of the solitary tract. J Neurophysiol. 2014; 111:1655–1670. [PubMed: 24381029]

Whitehead, MC. Gustatory. In: Watson, C.; Paxinos, G.; Puelles, L., editors. The mouse nervous system. San Diego, CA: Elsevier Academic Press; 2012. p. 571-588.

Whitehead MC, Bergula A, Holliday K. Forebrain projections to the rostral nucleus of the solitary tract in the hamster. J Comp Neurol. 2000; 422:429–447. [PubMed: 10861518]

Wilson DM, Boughter JD Jr, Lemon CH. Bitter taste stimuli induce differential neural codes in mouse brain. PLoS One. 2012; 7:e41597. [PubMed: 22844505]

Wilson DM, Lemon CH. Temperature systematically modifies neural activity for sweet taste. J Neurophysiol. 2014; 112:1667–1677. [PubMed: 24966301]

Yamaguchi S. Basic properties of umami and effects on humans. Physiol Behav. 1991; 49:833–841. [PubMed: 1679557]

Yamamoto T, Matsuo R, Fujimoto Y, Fukunaga I, Miyasaka A, Imoto T. Electrophysiological and behavioral studies on the taste of umami substances in the rat. Physiol Behav. 1991; 49:919–925. [PubMed: 1653433]

Yamamoto T, Sawa K. Comparison of c-Fos-like immunoreactivity in the brainstem following intraoral and intragastric infusions of chemical solutions in rats. Brain Res. 2000; 866:144–151. [PubMed: 10825490]

Yamamoto T, Shimura T, Sakai N, Ozaki N. Representation of hedonics and quality of taste stimuli in the parabrachial nucleus of the rat. Physiol Behav. 1994; 56:1197–1202. [PubMed: 7878091]

Yamamoto T, Yuyama N, Kato T, Kawamura Y. Gustatory responses of cortical neurons in rats. II. Information processing of taste quality. J Neurophysiol. 1985; 53:1356–1369. [PubMed: 4009223]

Yasumatsu K, Ogiwara Y, Takai S, Yoshida R, Iwatsuki K, Torii K, Margolskee RF, Ninomiya Y. Umami taste in mice uses multiple receptors and transduction pathways. J Physiol. 2012; 590:1155–1170. [PubMed: 22183726]

Yokota T, Eguchi K, Hiraba K. Topographical representations of taste response characteristics in the rostral nucleus of the solitary tract in the rat. J Neurophysiol. 2014; 111:182–196. [PubMed: 24133228]

Zaidi FN, Krimm RF, Whitehead MC. Exuberant neuronal convergence onto reduced taste bud targets with preservation of neural specificity in mice overexpressing neurotrophin in the tongue epithelium. J Neurosci. 2007; 27:13875–13881. [PubMed: 18077699]

Zhang F, Klebansky B, Fine RM, Xu H, Pronin A, Liu H, Tachdjian C, Li X. Molecular mechanism for the umami taste synergism. Proc Natl Acad Sci U S A. 2008; 105:20930–20934. [PubMed: 19104071]

Zhao GQ, Zhang Y, Hoon MA, Chandrashekar J, Erlenbach I, Ryba NJ, Zuker CS. The receptors for mammalian sweet and umami taste. Cell. 2003; 115:255–266. [PubMed: 14636554]

Highlights

- The majority of sweet-sensitive neurons possessed an umami synergistic response.
- Sucrose elicited greater response in the medial and BC than in the lateral division.
- Neurons in the lateral division possessed the greatest response to quinine.
- The proportion of neuron types in the medial vs. lateral divisions was different.
- PbN neurons appear to be more narrowly tuned when estimated by noise-to-signal (N/S) ratio than by entropy (*H*).

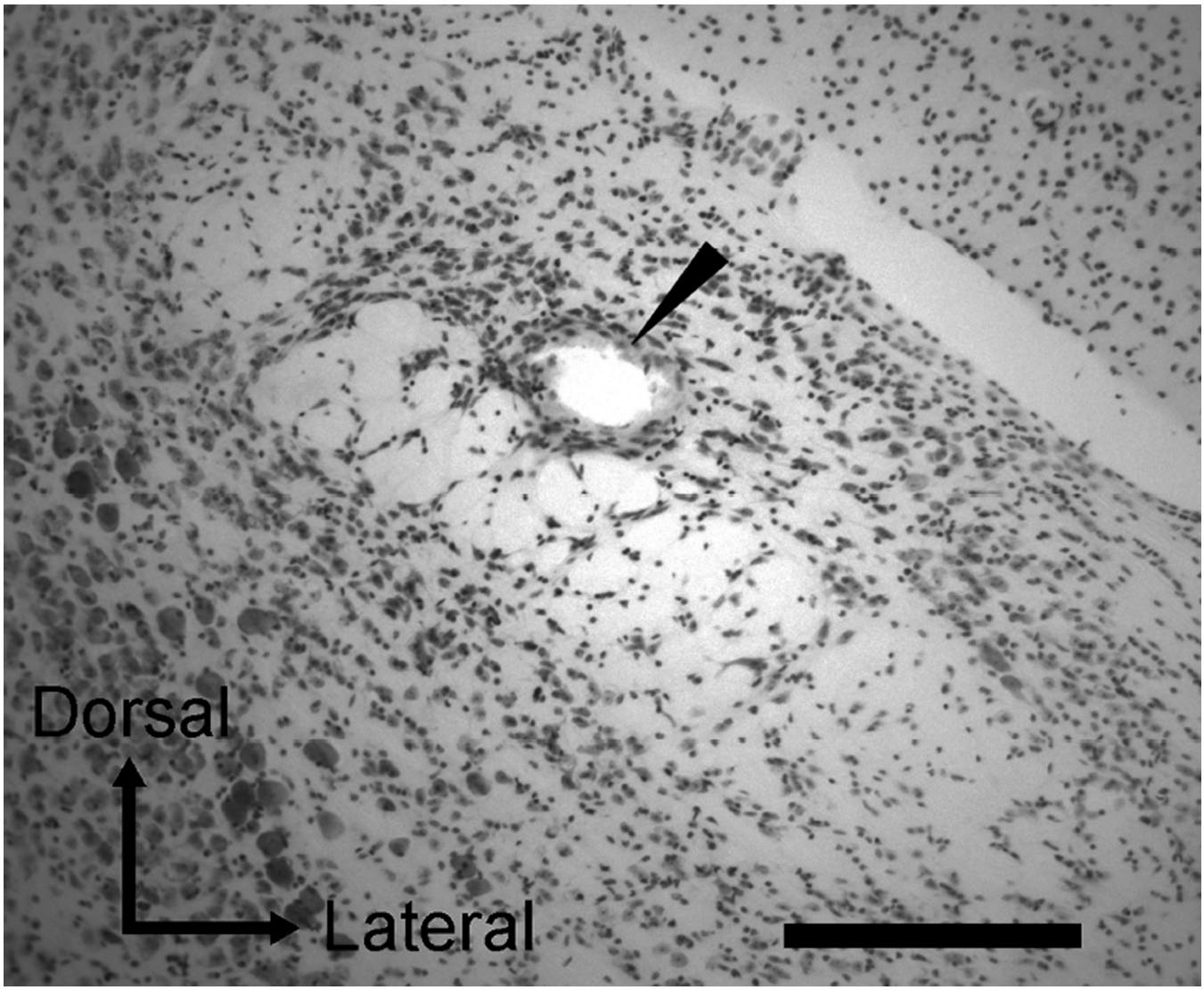

Figure 1.
Photomicrograph of a cresyl violet-stained section in the PbN. Marking lesion in the ventral lateral subnucleus is indicated by an arrowhead in this section. Scale bar = 500 μm.

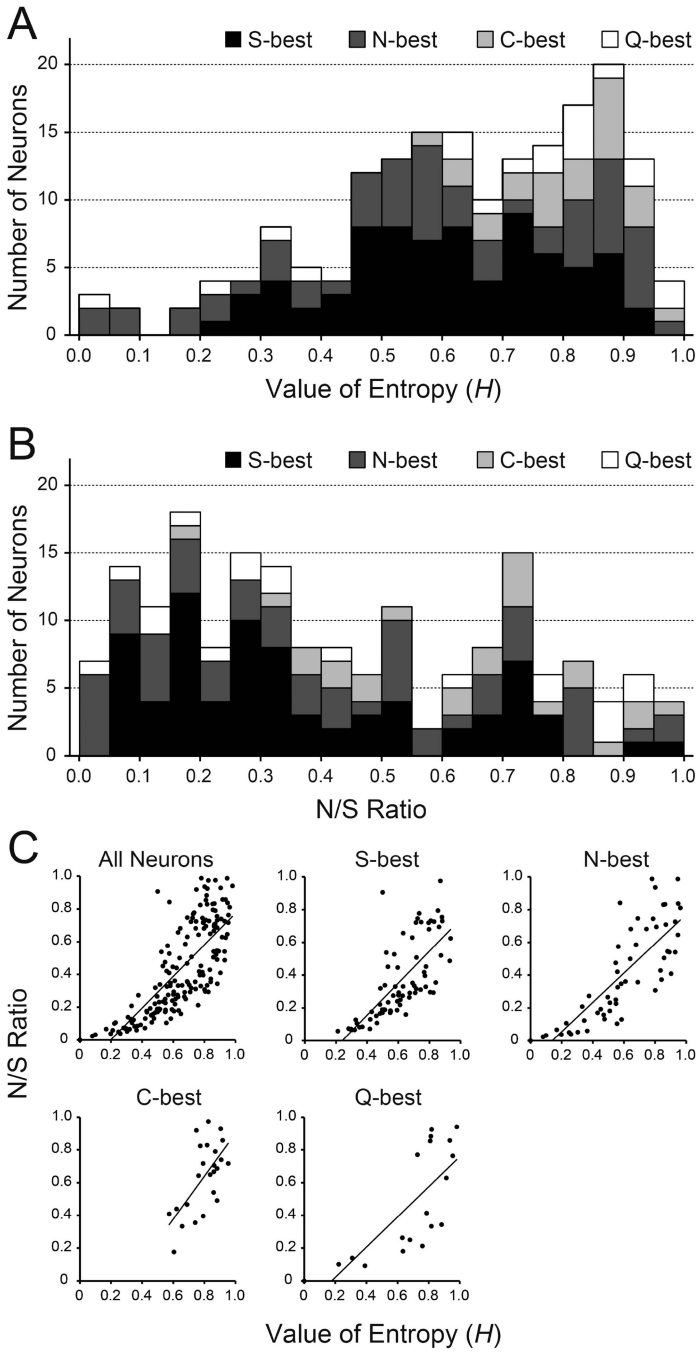

Figure 2.

A: Distribution of entropy values (*H*) of all 178 neurons categorized based on their best stimulus (range: 0.0 to 0.98). B: Distribution of noise-to-signal (N/S) ratio of all 178 neurons categorized based on their best stimulus (range: 0.0 to 0.98). C: Correlation between *H* and N/S ratio. Correlation coefficients for all neuron types, S-best, N-best, C-best and Q-best neurons were 0.78, 0.73, 0.82, 0.65 and 0.75, respectively.

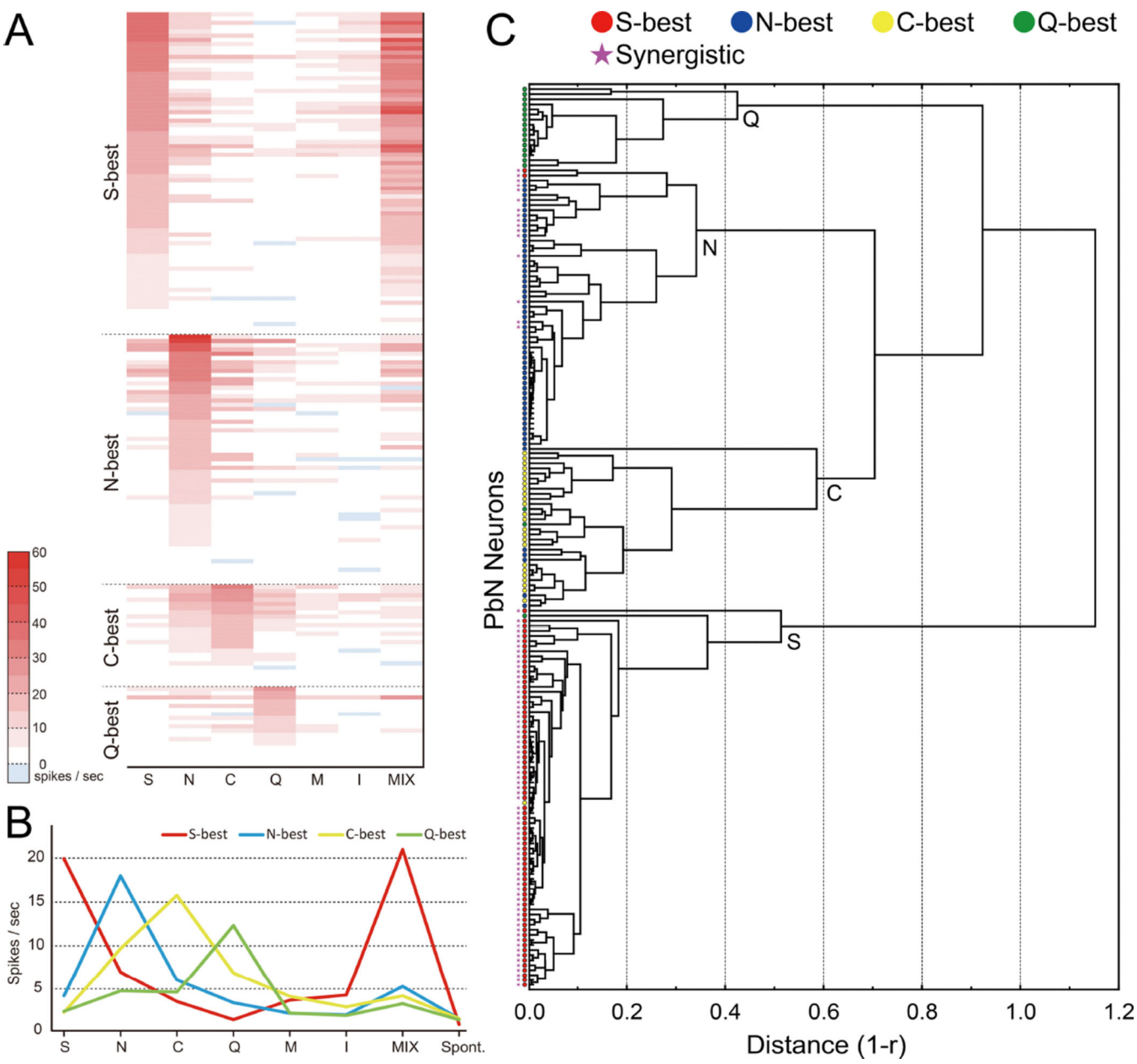

Figure 3.

Taste response profile A: Heat map showing responses of 178 PbN neurons to taste stimuli. Response profiles of PbN taste neurons by heat map. Taste neurons were grouped into best-stimulus categories and arranged within those categories in descending order of response magnitude to the best-stimulus [n = 178; 76 sucrose (S)-best; 59 NaCl (N)-best; 24 citric acid (C)-best; 19 QHCl (Q)-best]. Taste responses are presented as net responses (i.e. responses to stimulus - responses to water). B: Mean net taste responses of each neuron type. C: Dendrogram showing neuronal grouping. Each symbols indicate the neuron type based on neuron's best stimulus (circle) and umami synergism (star).

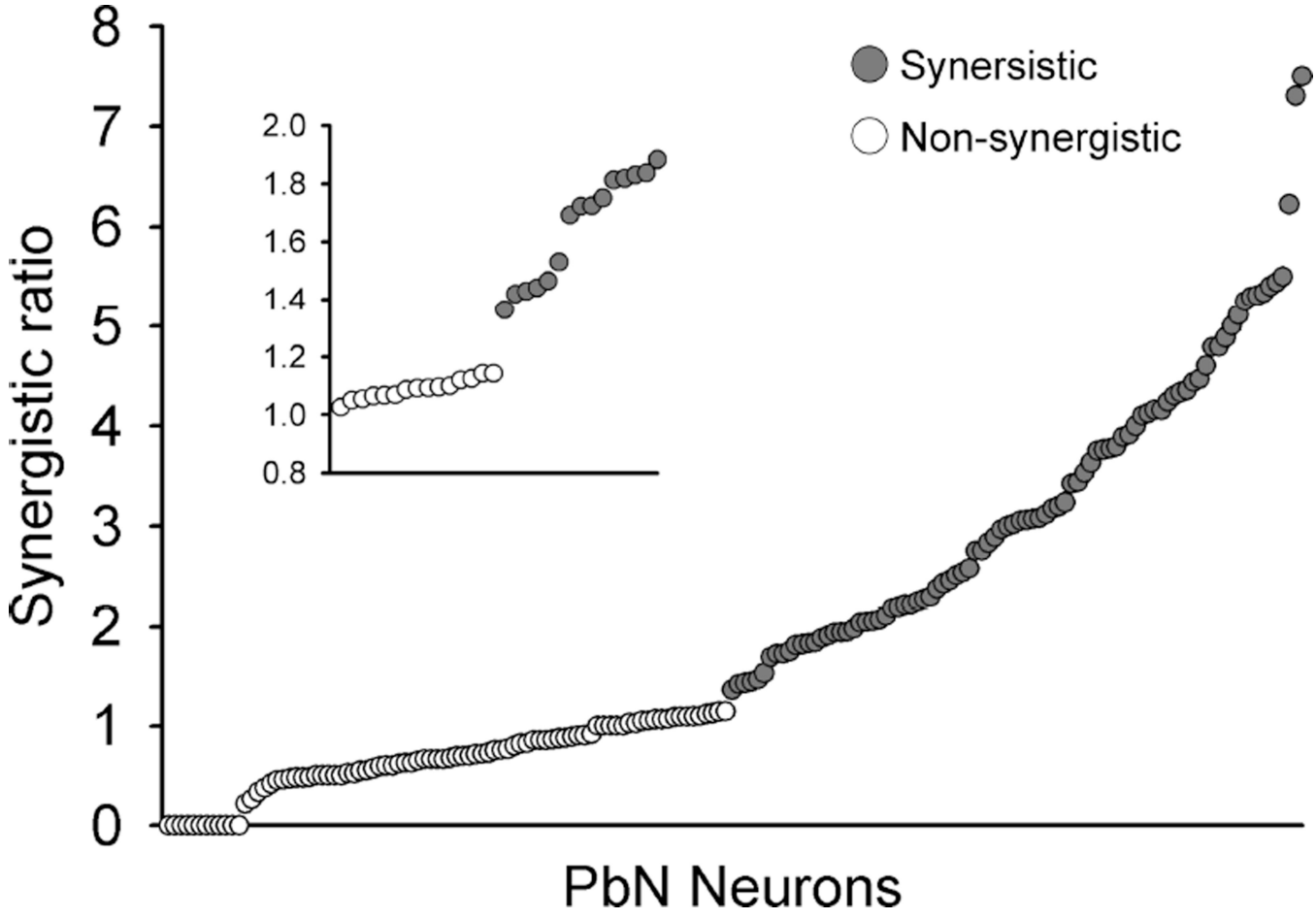

Figure 4.

Synergistic scores of synergistic (gray circles, n = 90) and non-synergistic neurons (open circles, n = 88). In the present study score 1.2 was used as a criterion to classify neurons into two groups, synergistic or non-synergistic (blown-up inset).

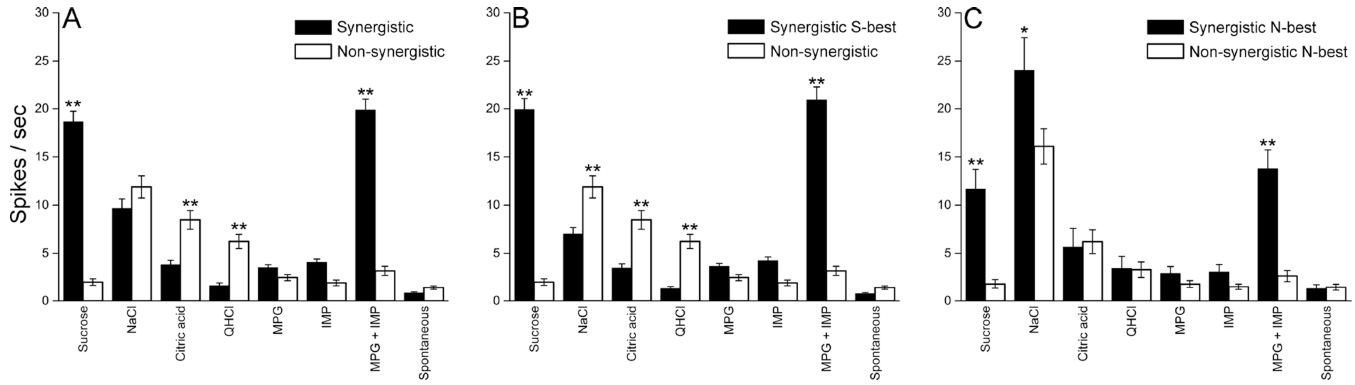

Figure 5.

A: Mean (±SEM) net taste responses and spontaneous activity of all synergistic (shaded bars, n = 90) and non-synergistic (open bars, n = 88) neurons. B: Mean (±SEM) net taste responses and spontaneous activity of synergistic S-best (shaded bars, n = 76) and all non-synergistic (open bars, n = 88) neurons. C: Mean (±SEM) net taste responses and spontaneous activity of synergistic N-best (shaded bars, n = 14) and non-synergistic N-best (open bars, n = 45) neurons. *$P < 0.05$, **$P < 0.01$.

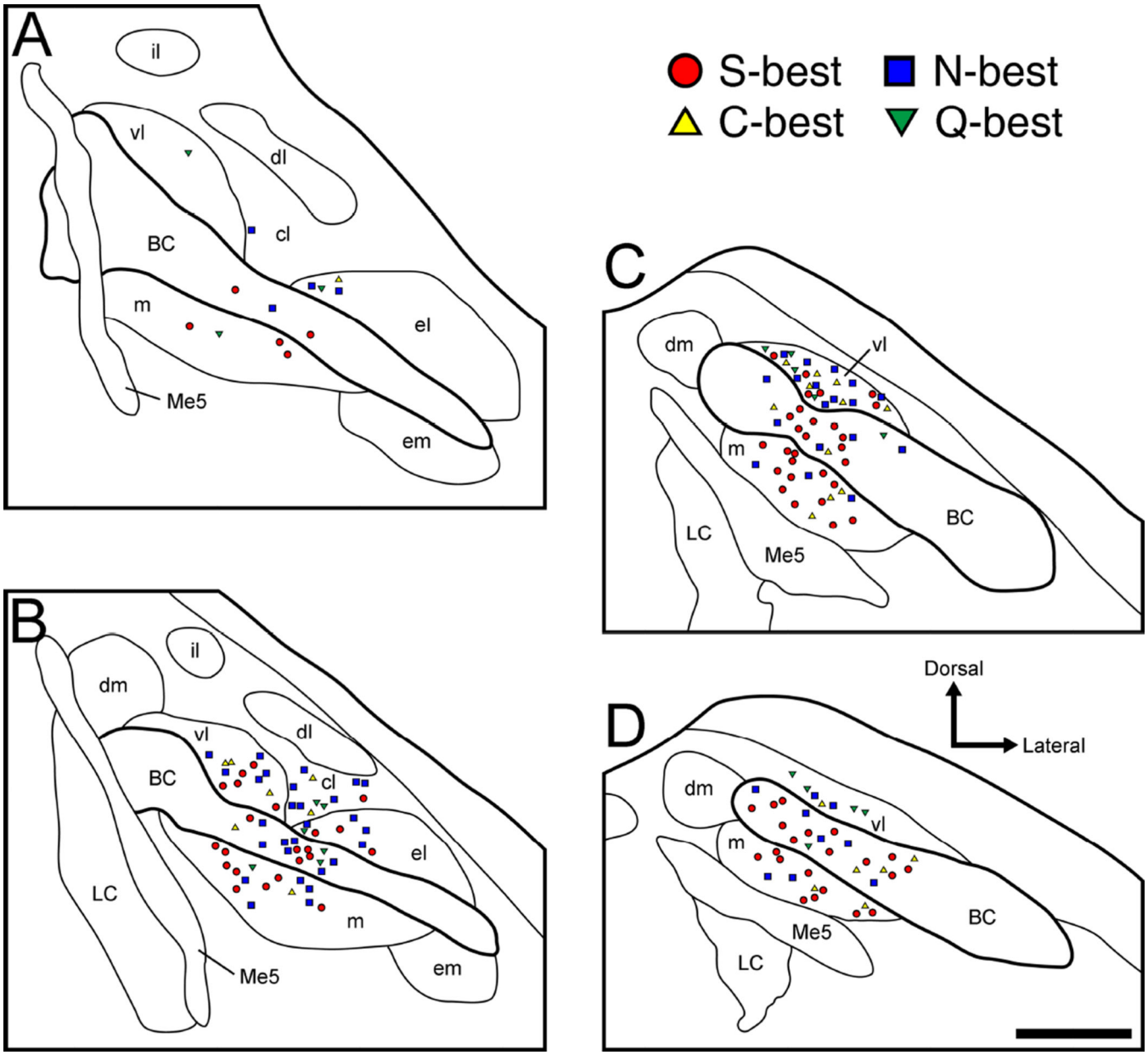

Figure 6.

Anatomical reconstruction of 178 recording sites in the right PbN in terms of best stimulus category. A–D: coronal sections are arranged rostral to caudal and +50, −100, −250, and −400 μm separated from the caudal end of the cuneiform nucleus, respectively. Filled symbols, synergistic units; open symbols, non-synergistic units; circles, S-best units; squares, N-best units; triangles, C-best units; inverted triangles, Q-best units. BC, brachium conjunctivum; cl, central lateral subnucleus; dl, dorsal lateral subnucleus; dm, dorsal medial subnucleus; el, external lateral subnucleus; em, external medial subnucleus; il, internal lateral subnucleus; LC, locus coeruleus; m, medial subnucleus; Me5, mesencephalic trigeminal nucleus; vl, ventral lateral subnucleus.

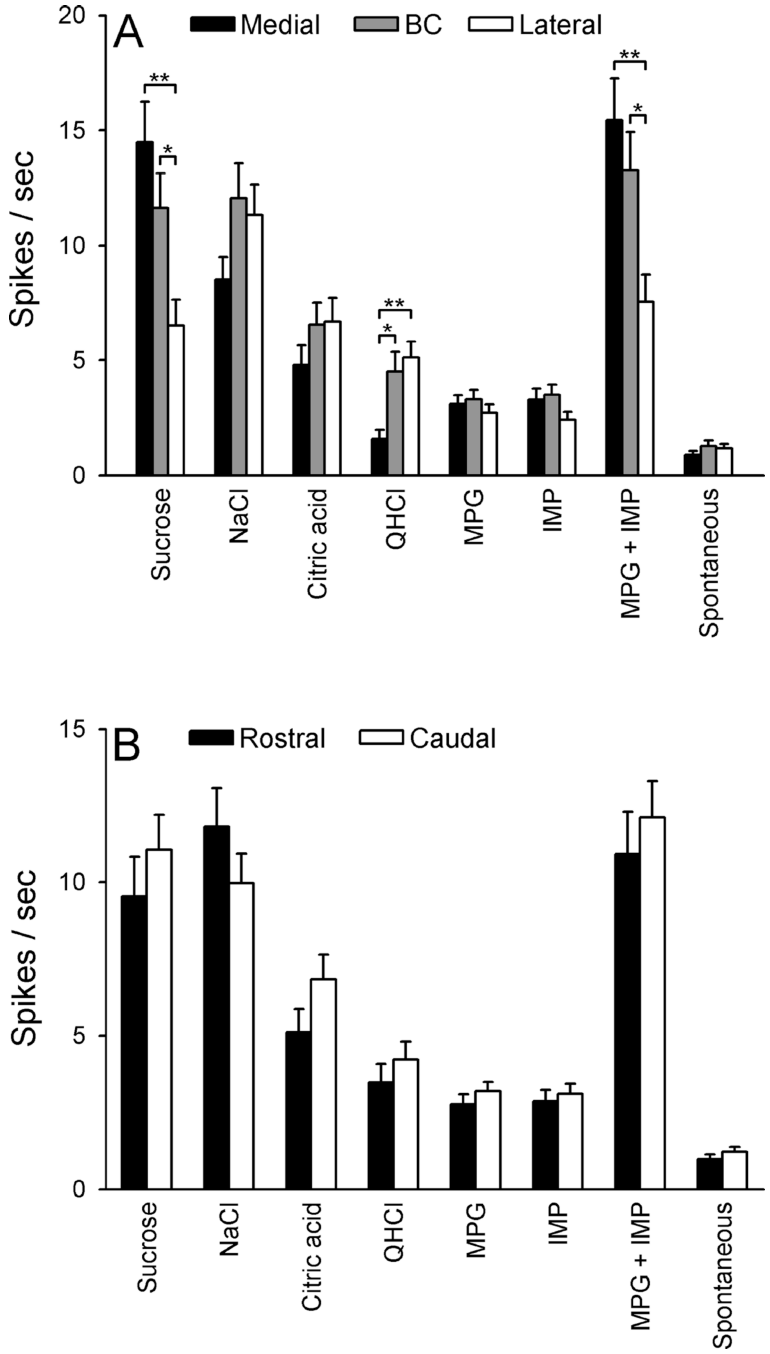

Figure 7.

A: Mean (± SEM) net taste responses and spontaneous activity of neurons recorded in the medial (n = 51), brachium conjunctivum [BC] (n = 56), and lateral (n = 71) subdivision of the PbN. B: Mean (± SEM) net taste responses and spontaneous activity of neurons recorded in the rostral (n = 75) and caudal (n = 103) subdivision of the PbN. *$P < 0.05$, **$P < 0.01$.

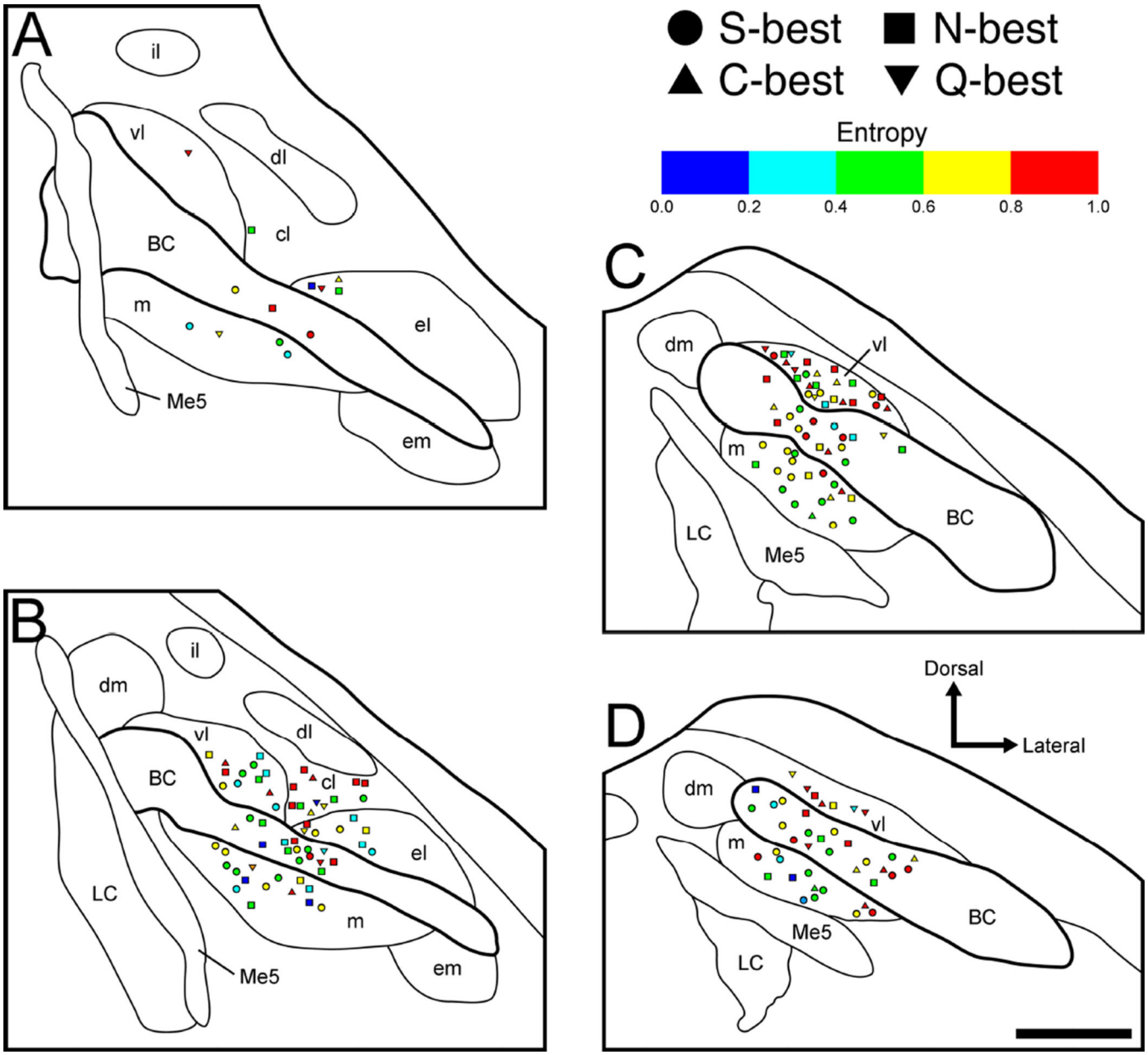

Figure 8.

Anatomical reconstruction of 178 recording sites in the right PbN in terms of entropy values (*H*) and best stimulus category. A–D: coronal sections are arranged rostral to caudal and +50, −100, −250, and −400 μm separated from the caudal end of the cuneiform nucleus, respectively. S-best units; squares, N-best units; triangles, C-best units; inverted triangles, Q-best units. BC, brachium conjunctivum; cl, central lateral subnucleus; dl, dorsal lateral subnucleus; dm, dorsal medial subnucleus; el, external lateral subnucleus; em, external medial subnucleus; il, internal lateral subnucleus; LC, locus coeruleus; m, medial subnucleus; Me5, mesencephalic trigeminal nucleus; vl, ventral lateral subnucleus.

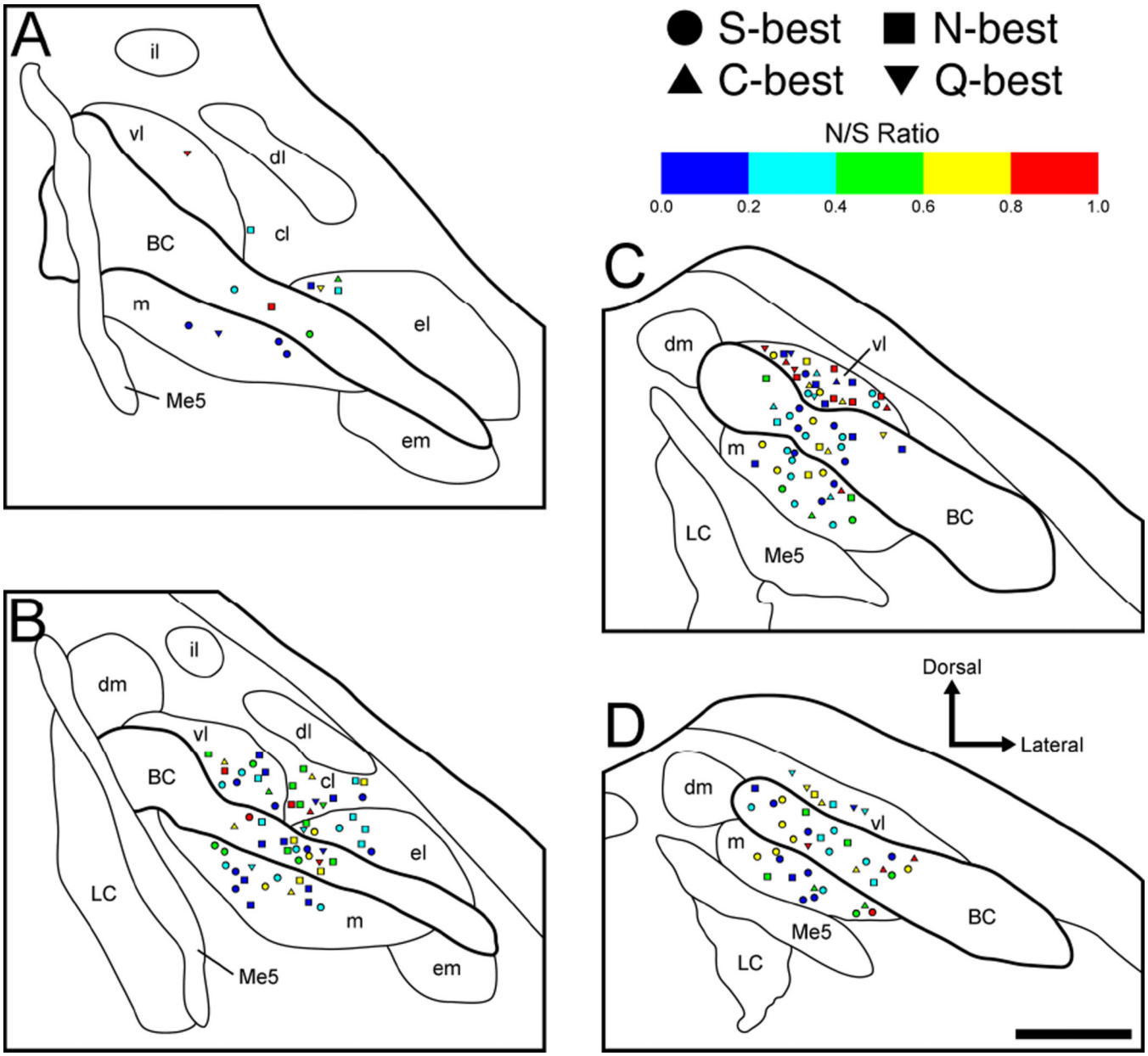

Figure 9.

Anatomical reconstruction of 178 recording sites in the right PbN in terms of noise-to-signal (N/S) ratio and best stimulus category. A–D: coronal sections are arranged rostral to caudal and +50, −100, −250, and −400 μm separated from the caudal end of the cuneiform nucleus, respectively. S-best units; squares, N-best units; triangles, C-best units; inverted triangles, Q-best units. BC, brachium conjunctivum; cl, central lateral subnucleus; dl, dorsal lateral subnucleus; dm, dorsal medial subnucleus; el, external lateral subnucleus; em, external medial subnucleus; il, internal lateral subnucleus; LC, locus coeruleus; m, medial subnucleus; Me5, mesencephalic trigeminal nucleus; vl, ventral lateral subnucleus.

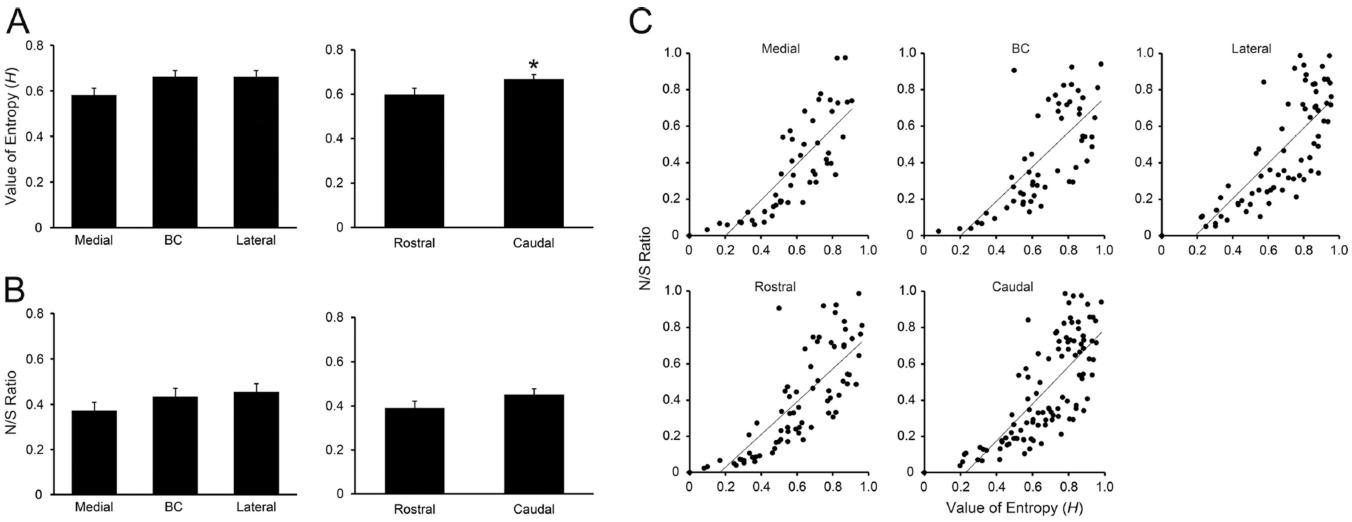

Figure 10.

A: Mean (± SEM) entropy values (*H*) of neurons recorded along with mediolateral (left) and rostrodaucal (right) axis in the PbN. B: Mean (± SEM) noise-to-signal (N/S) ratio of neurons recorded along with mediolateral (left) and rostrodaucal (right) axis in the PbN. **P* < 0.05. C: Correlation between *H* and N/S ratio. Correlation coefficients between *H* and N/S ratio for neurons recorded in the medial, BC, lateral, rostral and caudal subdivisions were 0.80, 0.73, 0.79, 0.79 and 0.76, respectively.

Table 1

Mediolateral location of recording site of neurons in terms of best stimulus

	Recording site			
Neuron Type	**Medial**	**BC**	**Lateral**	**Total**
S-best	33	28	15	76
N-best	10	18	31	59
C-best	6	6	12	24
Q-best	2	4	13	19
Total	51	56	71	178

Fisher's exact probability test revealed that the proportion of neuron types in the medial vs. lateral and BC vs. lateral subdivisions was significantly different ($P < 0.01$).

Table 2

Rostrocaudal location of recording site of neurons in terms of best stimulus

	Recording site		
Neuron Type	**Rostral**	**Caudal**	**Total**
S-best	27	49	76
N-best	32	27	59
C-best	7	17	24
Q-best	9	10	19
Total	75	103	178

Fisher's exact probability test revealed no significant difference in the rostrocaudal distribution of each neuron type ($P = 0.08$).

Table 3

Mediolateral location of recording site of neurons in terms of entropy value (*H*)

	Recording site			
Entropy value	**Medial**	**BC**	**Lateral**	**Total**
0.00–0.19	3	2	2	7
0.20–0.39	6	5	10	21
0.40–0.59	17	14	13	44
0.60–0.79	18	16	18	52
0.80–1.00	7	19	28	54
Total	51	56	71	178

Fisher's exact probability test revealed that the proportion of neurons in the medial vs. lateral subdivision was significantly different ($P < 0.05$).

Table 4

Mediolateral location of recording site of neurons in terms of noise-to-signal (N/S) ratio

	Recording site			
N/S ratio	**Medial**	**BC**	**Lateral**	**Total**
0.00–0.19	19	14	17	50
0.20–0.39	11	15	19	45
0.40–0.59	10	8	9	27
0.60–0.79	9	13	13	35
0.80–1.00	2	6	13	21
Total	51	56	71	178

Fisher's exact probability test revealed no significant difference in the proportion of neurons (medial vs. BC, $P = 0.42$; medial vs. lateral, $P = 0.08$; BC vs. lateral, $P = 0.81$).

Table 5

Rostrocaudal location of recording site of neurons in terms of entropy value (*H*)

	Recording site		
Entropy value	**Rostral**	**Caudal**	**Total**
0.00–0.19	5	2	7
0.20–0.39	13	8	21
0.40–0.59	18	26	44
0.60–0.79	19	33	52
0.80–1.00	20	34	54
Total	75	103	178

Fisher's exact probability test revealed no significant difference in the rostrocaudal distribution of neurons in terms of entropy value ($P = 0.14$).

Table 6

Rostrocaudal location of recording site of neurons in terms of noise-to-signal (N/S) ratio

	Recording site		
N/S ratio	**Rostral**	**Caudal**	**Total**
0.00–0.19	23	27	50
0.20–0.39	18	27	45
0.40–0.59	15	12	27
0.60–0.79	12	23	35
0.80–1.00	7	14	21
Total	75	103	178

Fisher's exact probability test revealed no significant difference in the rostrocaudal distribution of neurons in terms of N/S ratio ($P = 0.43$).